Chapter 4

High Energy Density Capacitance Microgenerators

Igor L. Baginsky and Edward G. Kostsov

Additional information is available at the end of the chapter

http://dx.doi.org/10.5772/48524

1. Introduction

The problem of continuous production of energy sufficient for modern microcircuits with an almost unlimited service life should be related to searching for power sources in the ambient medium. The comparison of these sources shows that only solar energy and energy of mechanical vibrations of surfaces of various solids can be used for generation of electrical energy in the milliwatt or microwatt range, which is enough for powering these microcirquits.

A typical feature for most modern sources of mechanical vibrations (surfaces of solids) is moderate amplitudes ranging from 0.1 to 2.0 μm; the analysis of the frequency distribution of amplitudes shows that low frequencies (1–100 Hz) have the most power [1]. Examples are vibrations of various building structures: supports, bridges, roadbeds, building walls, etc.

There are numerous recent publications that describe the development of microgenerators of electrical energy, including microelectromechanical systems (MEMS generators) capable of converting mechanical energy from the ambient medium to electrical energy. A new term, "energy harvesting," was accepted [2–11]. MEMS generators can be fabricated in a single technological cycle with fabrication of the basic microcircuit. The problem of powering MEMS devices is recognized as one of the most important issues in modern microelectronics.

Electrostatic energy microgenerators seem to be the most suitable for this task, because fuel or chemical elements need to be refined or renewed, solar or thermo- elements are not suitable for all situations of MEMS operation, electromagnetic generators of energy are ineffective in the range of low-amplitude vibrations and small sizes of the transducers, while piezoelectric generators are ineffective at low frequencies of vibrations [12-14].

Electrostatic generators have been known for a long time. Their operation principle is based on the work of mechanical forces transferring an electrical charge against

electrostatic forces of attraction of unlike charges [15]. Depending on the method of generation and transportation of this charge, generators can be divided into two classes. In the first class, the charge generated by some external action, for instance, by an electric arc or friction, is transferred by a transporter: a belt (Van de Graaf generators) [15] or a disk (friction machines). In the second class, the charged plate of the capacitor moves. Depending on the presence or absence of a built-in charge in this capacitor such devices are classified as either electret [16,17] or capacitance generators , e.g., Toepler or Felichi machines [15].

For electrostatic capacitance machine (Fig.1a) the separation of the plates (vertical, i.e., out-of-plane, or lateral, i.e., in-plane) of the capacitor $C(t)$ initially charged from the voltage source V_0 up to the value $Q_0 = C_{max}V_0$ (where C_{max} is initial maximal value of capacitance) in the conditions of open circuit results in growth of voltage on the capacitor up to the value

$$V_{max} = V_{min}\, C_{max}/C_{min}. \quad (1)$$

Here for the case under consideration $V_{min}=V_0$. And, respectively, the energy of capacitor is changed from $W_{min} = C_{max}V_0^2/2$ to

$$W_{max} = \frac{C_{max}}{C_{min}} W_{min} = \eta W_{min} = \frac{Q_0^2}{2C_{min}}\ , \quad (2)$$

where $\eta=C_{max}/C_{min}$ is capacitance modulation depth.

The produced electric energy W_{max}-W_{min} is transferred to load R. After that, the capacitor plates return to the initial position and are charged by the voltage source, and the energy conversion process is repeated. The power developed by such a generator is $P=(W_{max}-W_{min})f$ (where f is the repetition frequency of conversion cycles), and the efficiency of energy conversion, i.e. the ratio of energy produced by the generator during the conversion period to energy losses during the same period, is η-1.

Drawbacks of capacitance machine are the necessity of powering the generator by voltage source V_0 once at each cycle of energy conversion to charge the capacitor $C(t)$ and also the need in use of the key, synchronized with the phase of $C(t)$ alteration, switching the capacitor to the voltage source V_0, in the open circuit, and to the load R.

For these reasons, the circuit shown in Fig. 1a had limited applications: only for generation of high voltages (up to several hundreds of kilovolts) in solving special engineering problems.

This type of generators is used in many electrostatic MEMS generators [1,12,18-23]. Their specific power is low not exceeding 1-10 μW/cm² because of high value of minimum interelectrode gap at low η. It is possible to increase the generator power by decreasing the gap between the electrodes, but it results in the rising probability of an electrical breakdown in the gap. Low value of specific power is the main drawback of these generators; another problem is the necessity of using DC voltage sources.

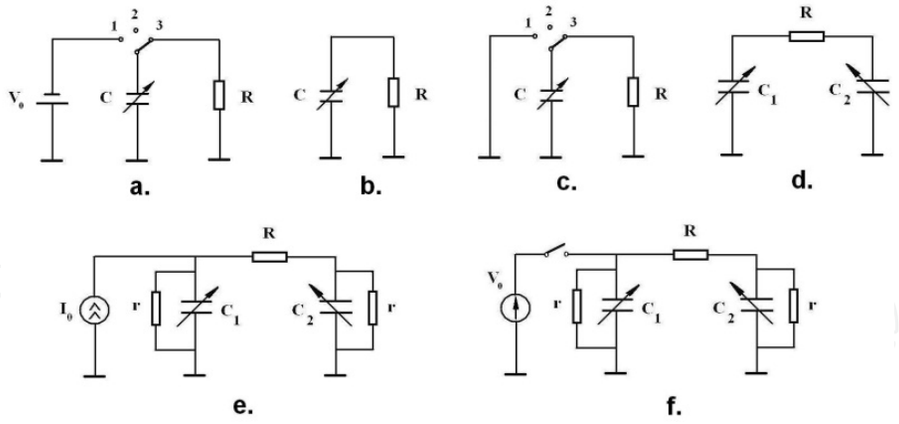

Figure 1. Various circuits of capacitance electrostatic generators: (**a**) capacitance machine; (**b**) electret current generator; (**c**) electret voltage generator; (**d**) ideal two-capacitor generator; (**e**) two-capacitor generator with loss compensation by a current source; (**f**) two-capacitor generator with loss compensation by a voltage source; V_0 is the voltage source, I_0 is the current source, R is the load resistance, and r is the leakage resistance.

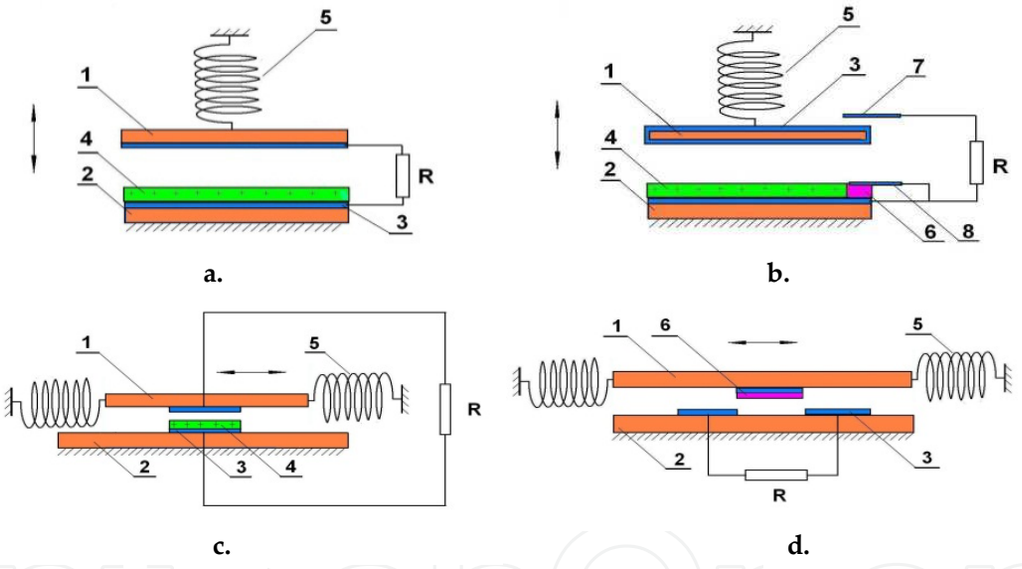

Figure 2. The schematic representation of the designs of capacitance generators, corresponding to the circuits presented on Fig.1: (**a**) – electret current generator, out-of-plane fabrication (see Fig.1b), (**b**) – electret voltage generator, out-of-plane plane fabrication (see Fig.1c), (**c**) – electret current generator, in-plane fabrication (see Fig.1b), (**d**) – two-capacitor generator, in-plane fabrication (see Fig.1d). 1 – moving substrate, 2 – stationary substrate, 3 – metal electrode, 4 – electret, 5 – spring, 6 – dielectric layer, 7 – contact 3 (Fig.1c), 8 – contact 1 (Fig.1c).

In electret generators [16,17,24-36] (see the circuits in Fig.1b,c and scematic designs in Fig.2a-c) the dielectric layer with built-in charge is formed on the inner surface of fixed plate of capacitor $C(t)$, and the charge losses are compensated by electrostatic induction of charge on the surface of moving plate, that is a considerable advantage of this way of energy transformation. These generators are further divided into current generators in which the capacitor $C(t)$ is directly connected to the load R (see Fig.1b and Fig.2a,c) and voltage generators in which the capacitor

C(t) is switched just like in capacitance machine but without the voltage source: *V=0*, Fig.1c and Fig.2b. Compared to voltage generators the current generators have the advantage in the simplicity of the circuit of energy transformation. The drawback is lack of the effect of generated voltage amplification, and correspondingly of the output power, proportional to capacitance modulation depth η. It should be noted that the "in-plane" constructions of electret generators (with lateral shift of the generator plate) having a comb structure of electrodes are being actively developed now. These devices are simple in production, and the technology earlier developed for smart sensors is used for their fabrication. For these devices the specific power of order 100 μW/cm² was reached [36]. The further increase of specific power is impeded by large interelectrode gaps used here, of order 20 μm.

The two-capacitor mode of capacitance energy transformation is described in [5,37,38], see Fig.1d and schematic design in Fig.2d. The electric energy is generated by means of capacitance alteration in antiphase of two capacitors ($C_i(t)$, $i=1,2$), initially charged to potential V_0, under the action of the force on their moving plates. In this case there is no need to feed the capacitors by switching on the voltage source on each cycle of energy transformation, because both capacitors C_i alternate in playing this role. The electric power is generated in the load R as the current flows from the recharging capacitors. If the generator has initial charge distributed between capacitances C_1 and C_2 then in idealized case with no leakage currents the circuit could operate for unlimitedly long time producing the energy under periodical action of mechanic force.

This approach has been proposed first in [37] as an idea. The evaluations of the efficiency of energy transformation were done in [5] taking into account the compensation of charge losses in the capacitors C_i by current source I_0, Fig.1e. However the total analysis of the generator operation at all possible loads and frequencies of generation, and at various ways of capacitance modulation and compensation of charge losses by connecting the current (Fig.1e) or voltage (Fig.1f) source have not been done.

The present work is aimed at performing the analysis of specific features of operation of electrostatic capacitance generators that do not need the electrical energy sources to compensate for charge leakages permanently, at each cycle of energy transformation. For the sake of generality only electric part of the generator will be analyzed under the modulation of capacitances of generating capacitors both by means of changes of interelectrode gaps and also by lateral shift of capacitors plates. A partial experimental verification of the results of the model proposed will be done.

2. High energy density electret generators

According to the common definition the ability of dielectric (or ferroelectric) to retain the charge produced in the bulk or on the surface of the layer by external action is called the electret effect. So we assume that this charge is constant in the time of generator action.

We will analyze first the vibration mode of this generator when the area of capacitor pates overlapping is constant and the distance between them is varied, or so called out-of-plane vibration mode.

The circuit of the generator considered is shown in Fig. 1, *b,c* and the schematic representation of their designs is represented in Fig.2 a,b. Its structure includes four thin layers: an electrode, a dielectric (ferroelectric) of thickness *d*, having a space charge ϱ(x,t), an air gap with a variable thickness $d_1(t)$ changing in time under the action of mechanical forces, and a moving electrode performing oscillatory motions with respect to the dielectric surface. In the general case, the operation principle of such an energy generator is the following. At *t=0* in each layer of the structure including the metallic electrodes the initial distribution of charge and corresponding distribution of electric field *E(x,0)* is set. The value of $E(x, t)$ is determined by the charge distribution in the dielectric layer and the voltage on the structure *V(t)*; the field in the electrodes is screened by the charge formed in them (Fig. 3).

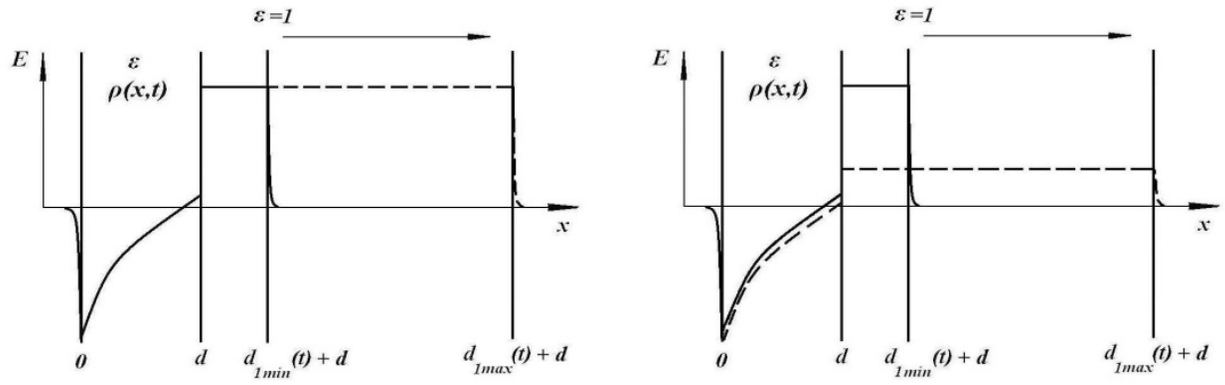

Figure 3. The schematic of the field distribution in the structure metal – dielectric with built-in charge – air gap – moving electrode at the initial state (solid lines) and in the phase of maximal plates shift (dashed lines): (**a**) – at the conditions of open circuit (voltage generator, fig.1c), and (**b**) – closed circuit (current generator, fig. 1b).

When the initial state is violated, i.e., the value of $d_1(t)$ is changed by mechanical forces, a redistribution of $E(x, t)$ occurs in each layer, accompanied by the current flow in the load circuit connecting the electrodes. When the current passes through the resistance *R*, the energy characterizing the energy parameters of the generator is released.

At the moment, the class of generators of electrical energy, which operate on the basis of the above mentioned principle, is well known; they are implemented in practice and are called electret generators [16]. The dielectric used in such generators belongs to a large group of materials that can retain the surface charge for a long time. The electrets [17] differ in the method of generation of this charge and in the form of the distribution of the stored charge and its sign. It can be either uniformly or nonuniformly distributed over the layer thickness and can have either an identical sign (monoelectret) or two different signs (geteroelectret). The electrets used in energy generators are sufficiently thick layers with the minimum thickness of 5–10 μm, and the information on their fabrication by microelectronics technologies is insufficient.

2.1. Model. Basic equations that describe the effect of energy generation in electrostatic machines with a dielectric containing an embedded charge

To describe the general features of operation of the generator considered, we assume that the dielectric contains a charge $\rho(x, t)$, which can change with time, with a surface density $Q_P(t) = \bar{\rho}(t)\bar{x}(t)$, where $\bar{\rho}(t)$ is the density of the space charge $\rho(x, t)$ averaged over the dielectric thickness and $\bar{x}(t)$ is its centroid.

Analyzing the behavior of the total current in this structure with variations of $d_1(t)$ for given values of d, $\bar{\rho}(t)$, $\bar{x}(t)$ we use a system of the classical one-dimensional equations consisting of the expressions for the total current $j(t)$ and conductivity current $j_c(x, t)$, equation of continuity, Poisson's equation, and expression that determines the potential V(t) between the electrodes at each instant of time. Taking into account that for electrets the space charge is constant for all time of the process, we have:

$$j(t) = \varepsilon\varepsilon_0 \frac{\partial E(x,t)}{\partial t} \tag{3}$$

$$\frac{\partial E(x,t)}{\partial x} = -\frac{\rho(x)}{\varepsilon\varepsilon_0} \tag{4}$$

$$\int_0^{d_1(t)+d} E(x,t)dx = -V(t) \ , \tag{5}$$

Integrating both parts of equation (4) with respect to the coordinate x, taking into account that the field increases in a jumplike manner by a factor of ε on the free boundary of the dielectric, i.e.,

$$\varepsilon E(d_-, t) = E(d_+, t) \ , \tag{6}$$

and substituting the formula derived for $E(x, t)$ into equation (5), we obtain expressions for the field on the boundaries $x = 0$ and $x = d_1(t) + d$: $E_c(t)$ and $E_A(t)$, and, correspondingly, for the specific charge induced on these boundaries:

$$Q_c(t) = -\varepsilon\varepsilon_0 E_c(t) = C(t)\left(V(t) + V_P\right) , \tag{7}$$

$$Q_S(t) = \varepsilon_0 E_A(t) = -C(t)\left(V(t) + V_P\right) , \tag{8}$$

$$C(t) = \frac{\varepsilon\varepsilon_0}{d + \varepsilon d_1(t)} \ , \tag{9}$$

$$V_P = \frac{Q_P}{C_F} \ , \tag{10}$$

where $C_F = \varepsilon\varepsilon_0/d$ is the specific capacitance of the dielectric layer.

Therefore, according to equations (3) and (8):

$$j(t) = \frac{dQ_S(t)}{dt} = -\frac{d}{dt}\left(C(t)(V(t) + V_P\right) \tag{11}$$

When the electrodes are connected via the load R and in the case of open circuit (as it is shown in Fig. 1c with the switch in position 3 and with the switch in position 2), the voltage behavior in time is described by following equations:

$$\frac{d}{dt}\left[C(t)\left(V(t) + V_P\right)\right] = -\frac{V(t)}{R} \tag{12}$$

$$\frac{d}{dt}\left[C(t)\left(V(t) + V_P\right)\right] = 0 \tag{13}$$

These equations with the corresponding initial conditions describe all possible regimes of operation of the electrostatic generator shown in Fig. 1 *b,c*.

To study specific features of its operation, we choose (without loss of generality) a sine law of variation of the gap size:

$$d_1(t) = d_{10}(1 + \alpha + \sin(\omega t)) \ , \tag{14}$$

$\omega=2\pi f$, $f=1/T$, T is the conversion cycle duration.

As has been shown in Introduction two types of generator construction, depending on the method of commutation of the switch (see Fig. 1 *b,c*), are possible in the case of motion of the moving electrode in the field of the space charge (or polarization) Q_P located in the dielectric. They have been called the voltage generator and the current generator.

2.2. Voltage generator in vibration mode

In such a generator, the output voltage is amplified compared to the case of current generator, which will be analized below in the section 2.3, in the following manner. At the initial state the capacitor electrodes are short-circuited by commutation of the switch to position 1 at the instant when the minimum distance between the surfaces of the moving electrode and dielectric is reached (see Fig. 1c and Fig.2b, the capacitance $C(t)$ has the maximum value at this instant). At the beginning of the process of electrodes separation the switch is turned to position 2; at the instant when the maximum value of $d_1(t)$ is reached, the switch is turned to position 3 and the energy worked out during the cycle is transferred to the load R.

Let us analyze the effect of voltage amplification in more detail. Under conditions of electrode motion with a non-closed circuit ($j(t) = 0$) and according to equation (13), we have

$$C(t)\left(V(t) + V_p\right) = const \ , \tag{15}$$

then

$$C_{\max}\left(V_{\min}+V_p\right)=C_{\min}\left(V_{\max}+V_p\right)\cdot \tag{16}$$

Therefore, we obtain

$$V_{\max}=\frac{C_{\max}}{C_{\min}}\left(V_{\min}+V_p\right)-V_p \tag{17}$$

Let the process of vibrations begin from the phase of the maximum convergence of the surfaces; then, in accordance with the initial condition $V(0) = V_{min}(0) = 0$, after the first displacement of the moving electrode to the maximum distance under the condition of open circuit (switch in position 2), we have

$$V_{\max}=V_p\left(\frac{C_{\max}}{C_{\min}}-1\right) \tag{18}$$

In this case, the following amount of energy is produced:

$$W=\frac{C_{\min}V_{\max}^2}{2}=\frac{C_{\min}V_p^2}{2}\left(\frac{C_{\max}}{C_{\min}}-1\right)^2\approx\frac{V_p^2}{2}\frac{C_{\max}^2}{C_{\min}} \tag{19}$$

The principle of mechanical energy conversion to electrical energy with electrode motion under the condition of an open circuit is illustrated by the distribution of the electrical field in the structure (Fig. 3a) both in the initial phase of motion $d_1 = d_{1min} = \alpha d_{10}$, and in the phase of the maximum distance of the electrode (anode) $d_1 = d_{1max} = 2d_{10} + d_{1min}$. As the electrode moves, the field in the gap remains constant, the total current equals zero, and the electrical field energy increases in accordance with the increase in the area under the curve $E^2(x)$, which is manifested as an increase in the difference in the potentials V between the electrodes (Fig. 4). The energy is transferred to the load R when the switch is turned to position 3. This transfer is efficient if R does not exceed the value $1/(2f\overline{C}S)$, where $\overline{C}$ is the cycle-averaged specific capacitance of the structure, S is the electrode area, and f is the frequency of vibrations.

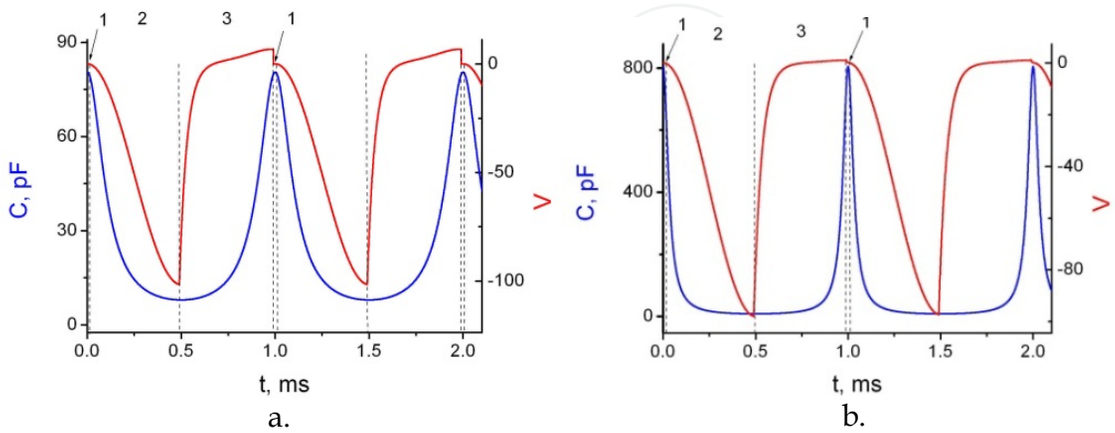

Figure 4. Behavior of $C(t)$ and $V(t)$ in a voltage electret generator based on (**a**) – dielectric: $Q_P = 10^{-3}$ C/m², $\varepsilon = 10$, and (**b**) – ferroelectric: $\varepsilon = 1000$ and $Q_P = 10^{-2}$ C/m². $d = 1$ μm, $d_{10} = 0.5$ μm, $d_{1min} = 10$ nm, $S = 1$ mm². $R = 10$ MΩ

In contrast to the capacitance machine where the energy transfer to the load is finalized at the end of the cycle by complete discharge of the capacitor $C(t)$ to $V(t) = 0$, the charge induced in the electrodes and screening the field of the space charge in the dielectric flows between the electrodes through the load R during the electrode motion in the generator considered here. This process is unsteady and is determined by several constants: instantaneous value of $RC(t)S$, time of the Debye screening of the charge in the metal (which is the smallest time), and time of motion of the moving electrode during the half-period. At certain times, depending on the relation between these time constants, the total current can change its direction, when the voltage also changes its sign at the instant of the maximum approaching of the surfaces ($d_1(t) \rightarrow d_{1\min}$) (see Fig. 4). To eliminate this effect, the switch (Fig.1c) is turned to position 1 at the beginning of each next cycle; then, the initial voltage $V_{\min} = 0$ is recovered, and the process is repeated completely.

Despite a principally different method of capacitance recharging, this circuit of energy conversion is similar to the capacitance machine (Fig. 1a), except for the fact that the field of the built-in charge inducing the voltage V_P serves here as the voltage source.

An universal program that takes into account all parameters of the structure and energy generation modes in the cases of one- and two-capacitor generator was developed for the numerical analysis of the problem. A difference scheme with automatic choice of the time step was used; this scheme ensured solution stability and specified accuracy.

One example of such a solution, which illustrates voltage generation between the electrodes for a particular dielectric with a low value of ε, is shown in Fig. 4a. The numbers on the axis t characterize the position of the switch (see Fig. 1c). It is seen from the figure that the role of this switch is the recovery of the initial state of the system ($V_{min} = 0$) in the phase when $C(t)=C_{max}$ in each cycle of energy generation. Such synchronization allows us to obtain the voltage amplification proportional to the capacitance modulation depth in accordance with (18); the power increases thereby in accordance with (19).

If a dielectric with a high value of ε is used in the generator, the capacitance modulation $C_{\max}/C_{\min}$ increases, but not in proportion to the increase in ε (when the air gap modulation depth is constant), because the value of $C_{\min}$ changes only slightly (it is determined by the maximum value of the air gap $2d_{10} + d_{1\min}$). In this case, with a fixed polarization Q_P , the value of V_P decreases inversely proportional to ε (10); the value of $V_{\max}$ (18) and also the energy generated in one cycle (19) decrease accordingly.

In particular, for the structure parameters used to construct the graphs in Fig. 4a, but with the value of ε increased by a factor of 100, the value of V_P decreases by a factor of 100, but the values of $V_{\max}$ and W decreases only by a factor of 10. Therefore, to reach the output voltage and the generated energy comparable with the case of the classical electret generator (with parameters corresponding to those in Fig. 4a), the polarization in the ferroelectric should be increased by ten times (up to 10^{-2} C/m^2) (Fig. 4b). Note that such values of polarization are not critical for a number of known ferroelectrics; therefore, it is possible to increase the amount of energy generated during one conversion cycle by the ferroelectric-based generator; this increase is limited only by the voltage of the breakdown in the gap

between the electrodes. Moreover, to increase the energy production, it is possible to use ferroelectrics with low values of ε and high values of spontaneous polarization, for instance, lithium niobate and tantalate (Q_P up to 0.5–0.8 C/m^2 with $\varepsilon \approx 40$) [39].

2.3. Current generator in vibration out-of-plane mode

The operation principle of the current generator is shown in Fig.1b and the example of its design is presented in Fig.2a, this scheme is the simplest among the other possible ones. In the case of structure capacitance modulation, the generator operates without voltage amplification [16].

There are publications on particular cases of the current generator, for instance, electret microphones [17] in which either the load resistance is small or the amplitude of electrode vibrations is small as compared with the air gap thickness. In this case, in accordance with the analysis performed above, we have $V << V_P$, and the current in the circuit is described as

$$j(t) = V_p \frac{dC(t)}{dt} \tag{20}$$

Let us consider the general solution of the problem of current generator operation with an arbitrary load, using equation (12) with the initial condition $V(0) = 0$ and with variation of the gap size in accordance with equation (14).

Equation (12) with provision for (14) is written in dimensionless form as

$$\frac{d\varphi(\tau)}{d\tau} = -\left(\frac{1+\alpha'+\sin\tau}{RC_1S\omega} - \frac{\cos\tau}{1+\alpha'+\sin\tau}\right)\varphi(\tau) + \frac{\cos\tau}{1+\alpha'+\sin\tau} \ , \tag{21}$$

where $\varphi = V/V_P$, $\tau = \omega t$, $\alpha' = \alpha + d/\varepsilon d_{10}$, and

$$C_1 = \varepsilon_0/d_{10} \tag{22}$$

is the specific capacitance at average value of the air gap. Therefore, the problem is determined only by two dimensionless parameters: α' and $RC_1S\omega$.

Note that with a sufficiently large air gap modulation depth, the parameter α' is inversely proportional to the structure capacitance modulation depth.

One example of the numerical solution of equation (21) is shown in Fig. 5. The initial increase in voltage during the first displacement of the moving electrode is similar to its increase in the voltage generator; it is determined by capacitance modulation and by the value of V_P (18). In subsequent periods of electrode motion, a quasi-steady screening charge is formed (it is described above), and the voltage amplitude V_m decreases; this amplitude becomes sign-variable and tends to $\pm V_P$ or to a smaller value, depending on the load resistance R. The time constant of the decrease in V_m is determined by the value of $R\overline{C}S$, where $\overline{C} \le C_1$ is the capacitance of the structure $C(t)$ (see the inset in Fig. 5) averaged over the period of vibrations.

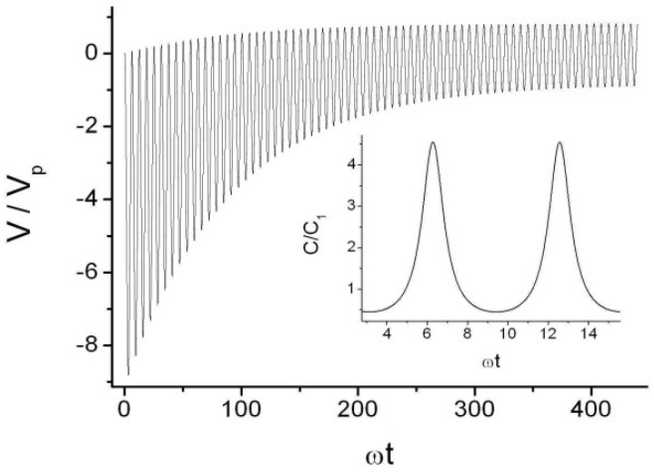

Figure 5. Transient of setting a steady state for the current generator at $\alpha' = 0.11$ and $\omega RC_1S = 1.11 \cdot 10^2$ ($Q_P = 10^{-3}$ C/m^2, $\varepsilon = 10$, $d = 1$ μm, $d_{10} = 1$ μm, $d_{1min} = 10$mn, $S = 1$ mm^2, $R = 20$ GΩ, and $f = 100$ Hz).

The specific features of the behavior of $V(t)$ in the steady regime are shown in Fig. 6. The change in the gap size $d_1(t)$ accompanied by the corresponding change in the capacitance $C(t)$ induces variations of the charge on the electrodes in time $Q_S(t)$; the maximum of this dependence in the general case can be shifted with respect to the peak value of the capacitance $C(t)$. This shift of the peaks of $Q_S(t)$ and $C(t)$ as compared with the classical case of the current generator considered in [16] (for which $V(t) = 0$ and equation (20) is valid) is caused by the delay in redistribution of the screening charge $Q_S(t)$ between the electrodes during current flow through the load R because of the finite value of $RC(t)S$.

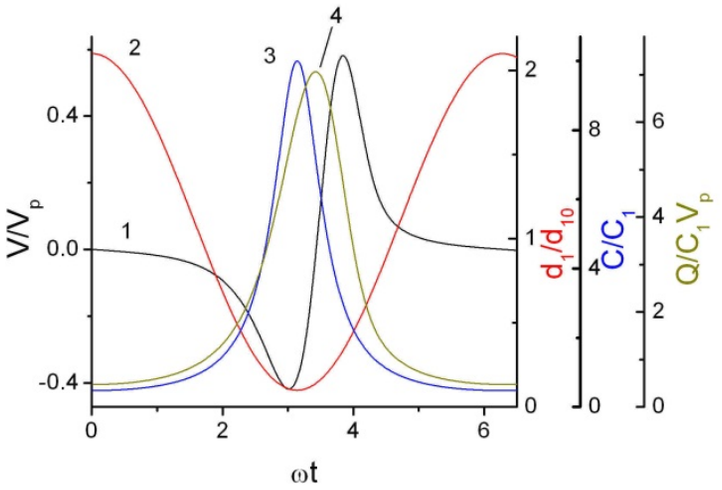

Figure 6. Example of the numerical solution of the equation that describes current generator operation in a steady regime with sinusoidal variations of the gap size d_1: V/V_P (*1*), d_1/d_{10} (*2*), C/C_1 (*3*), and Q_S/C_1V_P (*4*); $\alpha' = 0.1$ and $\omega RC_1S = 6.25\ 10^{-4}$.

The generator considered is qualitatively different both from the capacitance machine and from the voltage generator in one more operation principle: its operation is determined by changes in the conditions of screening of the electric field in metallic electrodes during the

motion of the moving electrode. The electrode recharging current in the circuit of the load R tends to return the system to the equilibrium state with $V = 0$.

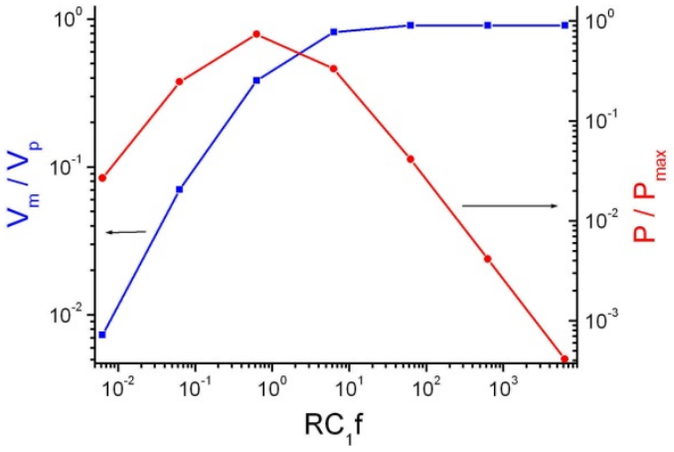

Figure 7. Frequency-load dependences of the produced power and output voltage for a current electret generator at $\alpha' = 0.1$.

If the structure capacitance modulation depth is sufficiently large, the amplitude of the voltage V_m produced by the generator tends (in the case of an optimal load) to the limiting value $\pm V_P$, and the power has the maximum value at the frequency

$$f_1 = 1/RC_1S, \tag{23}$$

as is shown in Fig. 7. Note that the law of current oscillations approaches the sine law as the parameter RC_1Sf increases to values of the order of unity and greater, in contrast to Fig. 6 where $RC_1Sf \ll 1$. Under these conditions, the power produced by the generator is $V_m^2/2R$. In the case of generation of the maximum power P_{max} at sufficiently large η, the value of V_m is close to V_P ; thus, we obtain

$$P_{\max} = \frac{1}{2}\frac{V_p^2}{R_m} = f\frac{C_1SV_p^2}{2}\ , \tag{24}$$

where $R_m = 1/(C_1Sf)$ is the load resistance at the generation of P_{max}. Correspondingly, the energy generated during the conversion period is expressed by

$$W_m = \frac{C_1SV_p^2}{2} \tag{25}$$

Thus, in the case of a sufficiently large depth of structure capacitance modulation, the amplitudes of power and the voltage of the current generator are almost independent of the values of C_{max} and C_{min}; they are determined only by the mean capacitance of the gap C_1.

Note that if $C_{max}/C_{min} > 5$ and $C_1/C_F < 0.1$ maximal output voltage approaches to V_P, and the maximum generated energy is given by (25).

2.4. Electret generator operation at lateral displacement of capacitor plates

The case of lateral displacement of capacitor plates under the operation of electret generator in the current mode (see the scematic design in Fig.2c) should be emphasized particularly, because it is realized in practice, see, e.g., so-called „in-plane gap-closing" constructions [32-36] and the rotational systems [29]. This operation mode is described by following equations (see equation (12)):

$$\frac{d}{dt}\left[CS(t)\left(V(t)+V_P\right)\right]=-\frac{V(t)}{R}\ , \tag{26}$$

where the area of the capacitor plates overlap is described as:

$$S(t)=S_{10}(1+\beta+\sin\omega t)\ , \tag{27}$$

and C is a specific capacitance, calculated by eqn. (9), which is constant in this case.

The equations (26) and (27) were solved numerically. The solution is represented in Fig. 8, where P_m is maximum value of power and P_{max} value is calculated using (24). This solution is qualitatively different from one for current out-of-plane electret generator, described above, by the presence of the pronounced dependence of output power on the modulation depth of structure capacitance, see Fig.8b, whereas in the previous case this dependence is practically not observed. Point is that in the case of lateral shift of capacitor plates the total value of polarization decreases along with the capacitance whereas in the previous case of vibration mode electret generator, for which the polarization is constant. The polarization decrease reduces in this time interval the influence of parazitic induced charge on the current, thus resulting in the effect of voltage amplification, as in the case of electret generator operation in the voltage vibratory mode. However, because the influence of the parazitic charge is not totally excluded, the value of maximum power P_m now is not proportional to capacitance modulation depth η (as for the case of capacitance machine) but P_m depends on η according to the logarithmic law, see Fig. 8b.

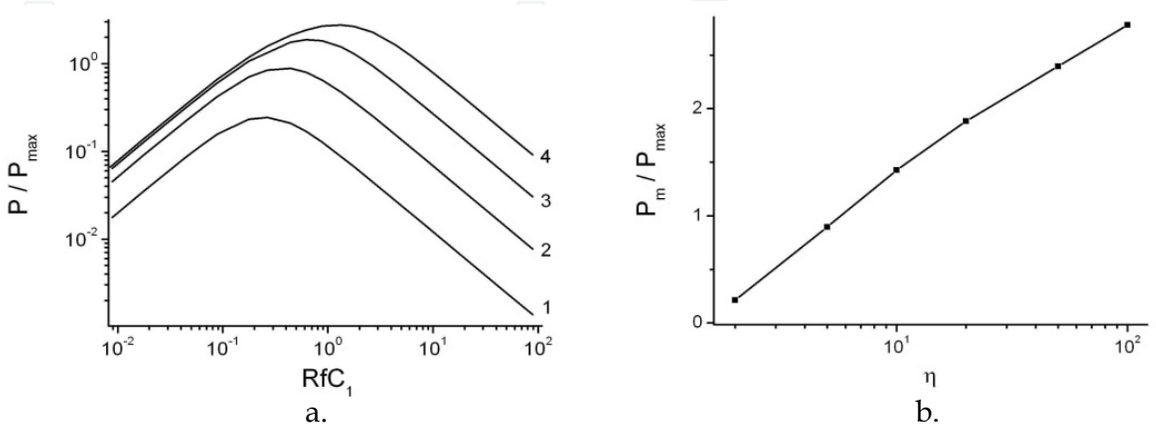

Figure 8. Electret generator with lateral shift of capacitor plates: (**a**) - frequency-load dependences of the output power for η = 2 (*1*), 5 (*2*), 20 (*3*), 100 (*4*) and (**b**) –the dependence of maximum power on capacitance modulation depth.

The drawback of this type of generator is the residual influence of parasitic induced charge mentioned above resulting in the reduction of the efficiency of the generation per unit area at equal parameters compared to out-of-plane generator in a current mode. In particular, the maximal output power of this generator becomes larger than that of its out-of-plane analog only for η>5.6, see Fig.8b. Inability to reach the small values of interelectrode gaps at high enough areas of generator plates should be marked as another drawback. These defects do not permit to reach high values of specific powers at η increase.

Note, that under transition in voltage generator mode the effects similar to those discussed in section **2.2** are observed. Therefore, in this mode the value of P_m/P_{max} will be proportional to capacitance modulation depth, and output power could be increased considerably.

3. Analysis of possible versions of implementation of two-capacitor generator circuits

Various versions of implementation of two-capacitor generators are based on the ideal generator circuit shown in Fig. 1d. They differ only in the method of compensation of charge losses caused by leakage currents in the generator capacitors (Fig. 1e,f).

Such compensation can be provided by an external source of electric energy. In the first case, a current source, i.e., a source that provides constant current and has a sufficiently high (in the ideal case, infinite) internal resistance, is connected to one of the generator capacitors (see Fig. 1e).

In the case of compensation of losses from the voltage source (whose internal resistance is low), it is necessary to use a switch connecting the source to one of the capacitors for a certain time sufficient for capacitor recharging (Fig. 1f).

Moreover, charge losses can be compensated by using an additional low-power generator connected to the input of the basic generator and consuming a minor portion of mechanical energy of the system, for instance, by using the electret effect [16].

It is also possible to compensate charge losses by organizing a feedback for transferring some part of energy from the generator output to its input for charging one of the capacitors, as shown in [10].

3.1. Compensation of charge losses with the use of a current source

The circuit based on this principle is shown in Fig. 1e. Operation of this generator is described by the system of differential equations

$$\begin{aligned} I(t) &= (V_2(t) - V_1(t)) / R; \\ I(t) &= -I_0 + \frac{d(V_1(t)C_1(t))}{dt} + \sigma_1(t)V_1(t); \\ I(t) &= -\frac{d(V_2(t)C_2(t))}{dt} - \sigma_2(t)V_2(t); \end{aligned} \tag{28}$$

where $V_1(t)$ and $V_2(t)$ are the drops of voltage on capacitors C_1 and C_2, respectively; $\sigma_1(t)$ and $\sigma_2(t)$ are the conductivities arising owing to leakages in these capacitors (in the general case, they are time-dependent).

Two operation modes of two-capacitor generators are possible: with lateral shift of the plates (with variations of the electrode overlapping area, a particular case is the rotor-type generator) and with vertical out-of plane vibrations of the plates (with variations of the interelectrode gap, vibrational mode). To obtain the maximum efficiency of energy generation, the capacitor plates move in the opposite phases in both cases.

3.1.1. Two-capacitor generator with lateral shift of the capacitors plates

This operation mode is demonstrated schematically in Fig.2d. In the case with capacitances changes in the opposite phases and with lateral shift of the capacitors plates, their total capacitance is constant:

$$C_1(t)+C_2(t)=C_0 \tag{29}$$

In a particular case, when the charge leakage is proportional to the electrode overlapping area, i.e., with similar changes in the conductivities, we have

$$\sigma_1(t)/C_1(t)=\sigma_2(t)/C_2(t) \tag{30}$$

In the case of constant leakages, we have

$$\sigma_1 = \sigma_2 = 1/r\ , \tag{31}$$

and for both cases

$$\sigma_1(t)+\sigma_2(t)=\sigma_0 \tag{32}$$

System (28) was solved numerically. In the dimensionless form system (28) was formulated in [5], and its solution is determined only by two dimensionless parameters characterizing the load properties of the system (fRC_0) and the charge losses due to leakage currents (fC_0/σ_0). By solving this system, we determined the voltages V_1 and V_2 on the capacitors C_1 and C_2, and also the corresponding charges $Q_1(t)$ and $Q_2(t)$, and the total charge $Q_\Sigma(t)$, the current $I(t)$ flowing through the load resistance R and the power released in this load resistance P, averaged over the time of the cycle of energy transformation T.

The system of equations that describes operation of the two-capacitor generator was analyzed in [5], where numerical solutions were obtained for the energy generation efficiency for various methods of excitation of shift vibrations of electrode grates. The output power generated by the generator, however, was not analyzed, and no analytical estimates were obtained.

Let us estimate the value of the maximum energy generated by this generator during one conversion cycle and, correspondingly, the power. As the first approximation, we consider the ideal two-capacitor generator (see Fig. 1d), which ensures minor leakages; therefore,

recharging of the capacitors (e.g., from a current source) is not needed. Let the generator capacitors be initially charged to a voltage V_0. Taking into account equation (29), we obtain

$$Q_0=C_0V_0= \text{const}, \tag{33}$$

where $Q_0 = Q_\Sigma(0)$ is the total initial charge accumulated on the capacitors. As there are no charge leakages in this case, the charge is retained during the entire time of generator operation.

Under the conditions described above, there is an initial segment of current relaxation with the characteristic time constant of the order of RC_0; during this time a dynamically equilibrium mode of generation is established owing to charge redistribution on the capacitors. The behavior of voltages on the capacitors depends in this case on the initial phases of $C_1(t)$ and $C_2(t)$. Other conditions are also possible, for instance, a gradual smooth increase in the amplitude and frequency of capacitance oscillations, which is closer to reality. We do not analyze this case in detail here, because the same dynamically equilibrium mode is established for all initial conditions.

Taking into account equations (1), (29) and (33) and also that $Q_0= C_{min}V_{max}+C_{max}V_{min}$, it is easy to get:

$$\frac{V_{\min}}{V_0} = \frac{1+1/\eta}{2}, \tag{34}$$

As both capacitors participate here in energy conversion, we can easily show that the energy W_2 produced during one conversion cycle is

$$\frac{W_2}{W_0} = \frac{P}{P_0} = \frac{\eta^2-1}{2\eta}, \tag{35}$$

$$W_0 = \frac{C_0 V_0^{\,2}}{2} \tag{36}$$

is initial energy accumulated in the capacitors and P is the power of the two-capacitor generator and $P_0 = W_0 f$. A comparison with one-capacitor generator (Fig.1a, energy W_1) results in the following expression

$$\frac{W_2}{W_1} = \frac{1}{2}\left(\frac{1}{\eta}+1\right)^2 \tag{37}$$

For $\eta >> 1$ we have

$$W_2 / W_1 \approx 1/2 \tag{38}$$

Thus, at identical initial voltages, the power provided by single-capacitor generator is twice as high as the maximum power of the two-capacitor generator. However, for the case of

one-capacitor generator the charge is completely consumed in each cycle of energy conversion, and it should be renewed, which makes this method of energy conversion more difficult in many cases. The power of the two-capacitor generator (with identical initial voltages) is lower because of the non-optimum incomplete charging of the capacitors C_i under the initial conditions mentioned above.

Solving system (28) with condition (29) numerically in the absence of charge leakages, we found the voltages on the capacitors Vi and then determined the current in the load resistance, the charge on the capacitors, and the generator power P. The dependence of P/P_0 on fRC_0, where $P_0 = fW_0$, is shown in Fig. 9.

The dependence of the maximum power P_{max}/P_0 on the modulation factor η (Fig. 10, curve 1) for the ideal generator is almost linear in the interval $\eta >> 1$ and is adequately described by (35) and curve 3 in Fig. 10. At small values of η, $1 < \eta < 3$, there are significant deviations from equation (35), because $V_{max}/V_{min} < \eta$ in this case and equation (1) is invalid.

With our method of normalization used here the curves in Fig. 9 depend only on the capacitance modulation factor. The curves in Fig. 10 are independent on the absolute parameters of the model, i.e., they have a universal character and describe all possible solutions of system (28) for the ideal generator case. From this viewpoint, we called them the "characteristic" curves.

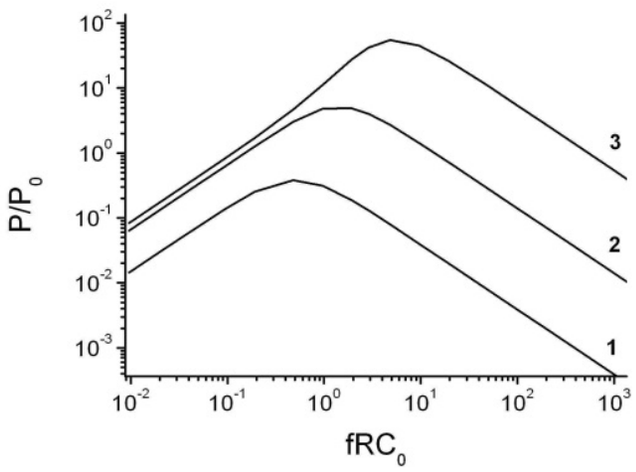

Figure 9. Characteristic curves of the generated power for the ideal generator: $\eta = 2$ (*1*), 10 (*2*), and 100 (*3*).

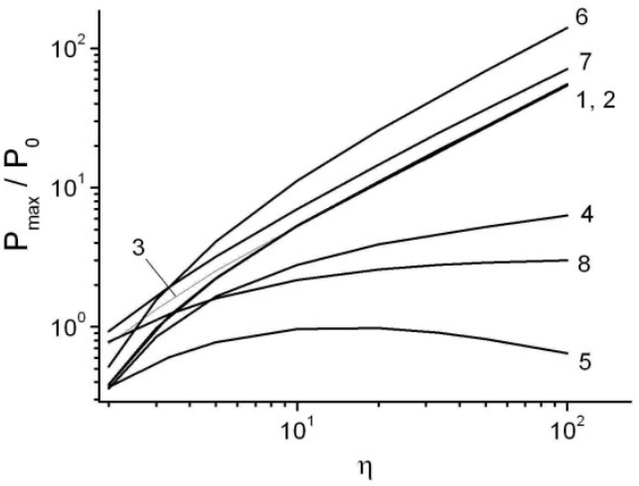

Figure 10. Characteristic curves of the maximum generated power P_{max}/P_0 versus the capacitance modulation factor for the following operation modes: ideal generator with lateral shift of the plates (*1*), lateral shift of the plates with modulation of charge leakages synchronized with capacitance modulation (*2*), lateral shift of the plates with constant leakages (*4*), out-of-plane antiphase vibrations of the plates (vibration generator) (*5*), lateral shift of the plates with recharging the capacitor C_1 from a voltage source under conditions $C_1(0) = C_{max}$ (*6*), out-of-plane antiphase vibrations of the plates for the ideal generator at $C_1(0) = C_{max}$ (*7*) and at $C_1(0)=C_2(0)$ (*8*), and analytical estimate for the ideal generator from equation (13) - (*3*).

An example of the numerical solution of (28) illustrating the operation of the two-capacitor generator in the absence of charge losses and with a set of parameters corresponding to its peak power is shown in Fig. 11.

Sinusoidal antiphase oscillations of the capacitors C_1 and C_2 lead to anharmonic oscillations of the charges Q_i potentials Vi, and also of the current I in the load resistance R. The greater the amplitude of oscillations of the values of V_i, Q_i, and I, the greater the generator power or its normalized value P/P_0 determined as W/W_0, i.e., the ratio of the energy produced by the generator during the period of oscillations to the initial energy accumulated on the capacitors:

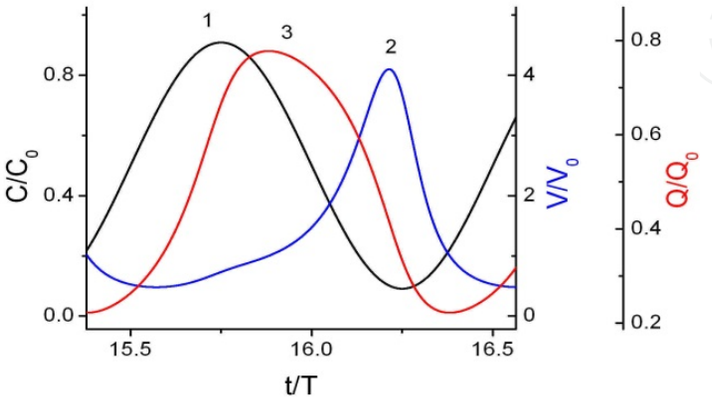

Figure 11. Time evolution of the capacitance (*1*), voltage (*2*), and charge (*3*) for one of the generator capacitors at the vicinity of optimum power ($\eta = 10$ and $fRC_0 = 1.9$).

$$P/P_0 = W/W_0 \ , \tag{39}$$

$$W = \int_{t_1}^{t_1+T} I^2(t)Rdt \ , \tag{40}$$

$P = Wf$ is the power.

Note that the results of the numerical analysis support the above-formulated approximation (1), from which it follows that the charges Q_i at the maximum and minimum values of the capacitance are equal, i.e., $C_{min}V_{max} = C_{max}V_{min}$ (see Fig. 11, curve *3*).

At sufficiently high frequencies ($f >> 1/RC_0$), the capacitors C_1 and C_2 do not have enough time to exchange the charge during one cycle of energy conversion, which reduces the charge modulation factor on each capacitor in the dynamically equilibrium mode. Therefore, the energy W generated during the cycle becomes smaller than the limiting value W_2. On the other hand, at low frequencies ($f << 1/RC_0$), energy conversion is also ineffective, because the charge passes to the second capacitor under these conditions faster than the capacitance of the generating capacitor reaches the minimum value. The charge on the capacitors "tracks" the changes in the capacitance. Thus, a typical feature of two-capacitor generators is the optimum of the normalized power P/P_0 in the frequency range $f \sim 1/RC_0$, which is consistent with the results of the numerical analysis (see Fig.9). Under the optimum generation conditions, as the capacitance of the generating capacitor (in which energy conversion occurs in the time interval considered) decreases, a significant portion of the charge flows to the other capacitor, thus, recovering the state corresponding to the beginning of generation on this capacitor. As the capacitance modulation factor η increases, the generator power P/P_0 also increases, and its peak is shifted toward higher frequencies.

Let us consider the operation of the two-capacitor generator taking into account the charge losses due to leakage currents and its compensation from an external current source. In the equivalent circuit shown in Fig. 1e, the charge losses are shown as conductivities $\sigma_i(t)$ connected in parallel to the capacitors $C_i(t)$. A d. c. current source I_0 is used for compensation of these losses. The operation of such a generator is described by the system of differential equations (28) with initial conditions corresponding to the steady state of the system with the current I_0 flowing in the circuit.

Solving this system numerically, we determined the dimensionless values of the potentials $y(x)$ and $z(x)$ on the capacitors C_i and then the quantities characterizing the generator operation.

Let us first analyze the case with capacitance and conductivity modulation in accordance with an identical sine law, i.e., when the conditions (29) and (30) are satisfied.

Such modulation of conductivities is typical for real situation when leakages are proportional to the area of overlapping of the capacitors plates. Subtracting the corresponding components of the third equation of system (28) from the left and right sides

of the second equation of the same system and taking into account equations (29,30,32) we obtain the expression of total charge:

$$\frac{dQ_{\Sigma}(t)}{dt} = -Q_{\Sigma}(t)\frac{\sigma_0}{C_0} + I_0 \tag{41}$$

Using the initial condition that describes the charge of the capacitors from the current source I_0 in the steady state: $Q_{\Sigma}(0)=I_0C_0/\sigma_0$ we can easily show that equation (41) has only one unique solution (Fig.12, curve 1)

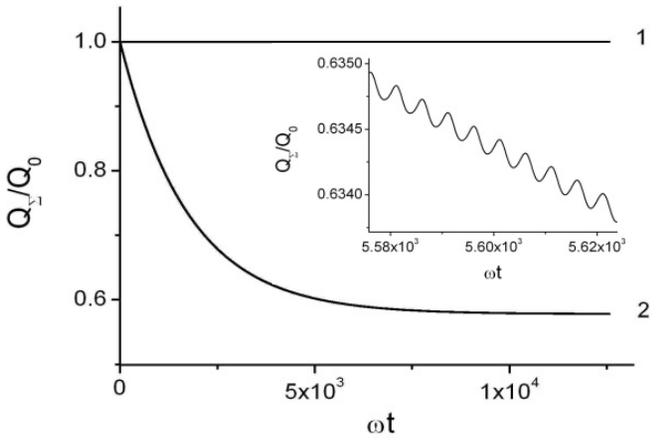

Figure 12. Time evolution of the total charge of the generator capacitances at $fRC_0 = 9.6$ and $\eta = 10$: modulation of leakages synchronized with modulation of the capacitances, equation (18)), - (*1*), and constant leakages (2) ($frC_0 = 9.6\ 10^2$). The inset shows a zoomed-in fragment of curve *2*.

$$Q_{\Sigma}(t) = Q_{\Sigma}(0) = \frac{I_0C_0}{\sigma_0} \tag{42}$$

Then, all estimates of the maximum energy produced by the ideal generator during the period of energy conversion and the estimates of the generator power are valid at a certain effective value of the initial voltage

$$V_0^* = I_0 / \sigma_0 \tag{43}$$

As an example, Fig. 10 shows the characteristic curve 2 of P_{max}/P_0 as a function of η, which completely coincides with curve 1 for the ideal generator. In the general case, the value of V_0^* is not equal to the real value of the initial voltage *V(0)*, because the value of *V(0)* depends on the initial phase of oscillations, i.e., on particular values of the conductivities σ_1 and σ_2 at the time $t = 0$.

The second case also observed in practice is the case with constant leakages:

$$\sigma_1(t) = \sigma_2(t) = \sigma_0 / 2 \tag{44}$$

A significant difference of this solution from the case of negligibly small leakage currents and also from the case of proportionality of the conductivity σ_i to the electrode overlapping area

considered above is the initial decrease in the total charge Q_Σ in time (see Fig. 12, curve 2) and its low-amplitude oscillations (see the inset in Fig. 12) in accordance with the period of changes in the capacitances C_i: $T = 2\pi/\omega$. This effect is explained by the increase in the leakage currents in each period owing to the increase in the potentials V_i on the capacitances, which leads to a certain decrease in the charges Q_i (later on, the charges Q_i again increase when the potentials V_i pass through their minimum values owing to recharging from the source I_0). At the initial stage of the process, the leakage currents averaged over the cycle of generation are greater than the source current I_0, and the discharge of capacitors takes place. For this mode, the steady-state value of the charge $Q_\Sigma(\infty)$ cannot be estimated analytically; therefore, the decay of the charge in time was analyzed numerically: it grows with increasing of both η and the absolute value of the capacitance. In most realistic cases, however, the decrease in the total charge $k = Q_\Sigma(0)/Q_\Sigma(\infty)$ is not more than a factor of 2.

Assuming that the total charge decreases by a factor of k and taking into account the expression for the initial charge (33), we can easily obtain expressions for steady-state values of the minimum voltage on the capacitors $V_{min}(\infty)$ and the energy produced by the generator $W(\infty)$. These formulas are completely identical to the expressions for the ideal generator (34-36) with V_0 being replaced by $V(\infty) = I_0/(k\sigma_0)$.

Thus, a typical feature of the two-capacitor generator with constant charge leakages is an additional decrease in the generated voltage by a factor of k and, correspondingly an additional decrease in power by a factor of k^2, as compared with the above-described case where the leakages are proportional to the electrode overlapping area (30). The dependence of the power P/P_0 on fRC_0 is qualitatively similar to the corresponding curves for the ideal generator with the only difference that it is additionally affected by the leakage currents (parameter frC_0): it increases linearly with decreasing leakages at a constant current I_0. In our scales, the value of P/P_0 is almost independent of frC_0 if the leakages are sufficiently small: $r \ll R$ (Fig. 13). As for the ideal generator, we see that P_{max}/P_0 increases with increasing capacitance modulation factor η and then reaches a "plateau" (see Fig. 10, curve 4). The frequency dependence of the power is qualitatively similar to the corresponding characteristic of the ideal generator.

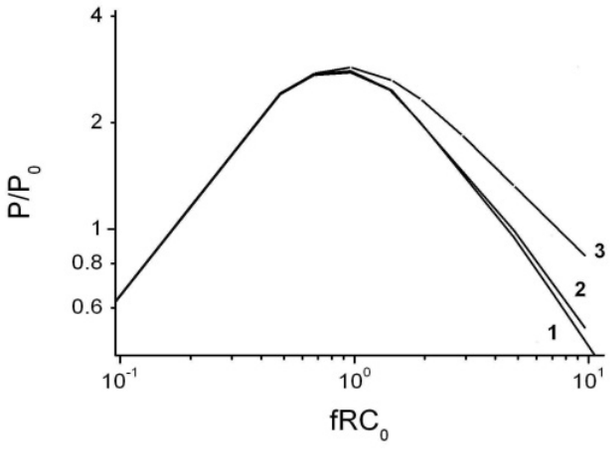

Figure 13. Characteristic curves of the generator power for different leakage resistances r: frC_0 = 960 (*1*), 96 (*2*), and 9.6 (*3*); η = 10.

The decrease in the total charge (see Fig. 12) and the generated power, which is determined by the charge redistribution after generator actuation at the beginning of modulation of the capacitances C_i, has an exponential character. The time needed for the generator to reach a steady-state mode is inversely proportional to the conductivity of the leakage currents. As energy generation is efficient only at $r >> R$ [5], and the time constant of the decrease in power τ has the order of $rC_0/2$, this time can be sufficiently large (more than 10^2–10^3 s). Note that the quasi-steady mode of generator operation is not reached under real conditions (e.g., in the regime of harvesting the energy of microvibrations of environment) where the modulation frequencies change in a shorter time than τ; therefore, the maximum of the generated power lies between curves 1 and 4 in Fig. 10.

3.1.2. Two capacitor generator in vibration out-of-plane mode

If the two-capacitor generator works at the interelectrode gap modulation mode, when the electrode overlapping area remains constant, called "mode of vibrations", then the condition of the constant total capacitance of the capacitors in time (29) is not satisfied. In this case, the gaps of two capacitors are modulated in opposition in accordance with a sinusoidal law, while the capacitance of each capacitor is inversely proportional to the gap value (Fig. 14, curves 1 and 1′; the quantity C_0' has the meaning of a capacitance averaged over the period of vibrations). Therefore, the capacitance of each capacitor is close to the minimum value during the major part of the period of vibrations T. The greater the capacitance modulation factor η, the more pronounced this effect: when the plates of one capacitor become separated (curve 1, motion toward decreasing $C_1(t)$) and the voltage on this capacitor increases accordingly (curve 2), the charge from this capacitor flows to the second capacitor whose capacitance $C_2(t)$ is still low (curve 1′). Thus, in contrast to the lateral shift of the plates, the charge overflow is not matched with the motion of the plates of the second capacitor: the peak of $V_1(t)$ occurs earlier than the peak of $C_2(t)$, i.e., the charge from the first capacitor flows to the second capacitor mainly during the time when its capacitance is close to the minimum value.

The absence of "synchronization" of the charge exchange between the capacitors in the generator in the mode of vibrations reduces the generator power (see Fig. 10, curve 5, P_0 is determined by equations (36) and (39), in which C_0 is replaced by C_0'), which is manifested as a decrease in the ratio V_{max}/V_0 (see Fig. 14, curve 2). Because of the lack of synchronization, there appears a second peak (with a lower amplitude) on the curve $V_1(t)$ after the peak on the curve $C_2(t)$, which also decreases the efficiency of generation in this mode.

Speaking about the generator in the vibration mode, we should emphasize the ideal generator mode (Fig. 10, curves 7, 8). In contrast to the mode of the lateral shift of the electrodes, the generated energy here depends appreciably on the initial values of the capacitances C_i. In particular, if the plates of one capacitor are located at the minimum distance at the beginning of the vibration process, then the maximum of energy generated in one cycle normalized to its initial value (Fig.10, curve 7) is greater than the value typical for the generator whose operation principle is based on the shift of the plates (Fig.10, curve 1). In

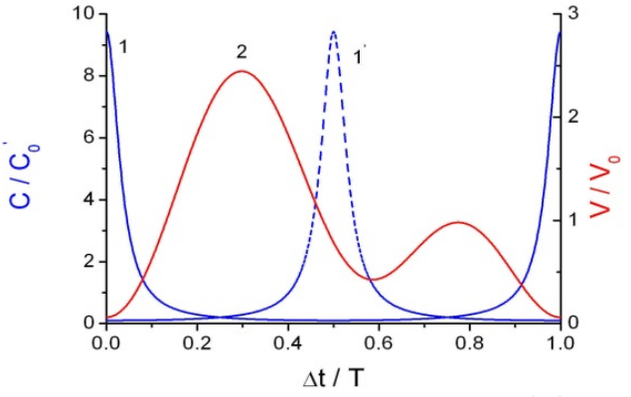

Figure 14. Time evolution of the capacitances of the first (*1*) and second (*1′*) capacitors and the voltage (*2*) for the first capacitor of the generator in the optimum power region. Mode of out-of-plane antiphase vibrations, $\eta = 10$, and $fRC_0 = 0.854$.

this case, the ultimate power for two capacitor generators is reached, because it is possible to ensure the minimum possible gaps between the electrodes of the generator capacitors and, therefore, the maximum possible values of the capacitance. However, if the beginning of the vibration process does not coincide with the instant when the maximum capacitance of one of the capacitors is reached, then the energy generation efficiency drastically decreases (Fig.10, curve 8). This behavior of the generated power is explained by the magnitude of the charge trapped at the beginning of the process: if one of the capacitances has the maximum value at the beginning of the process (Fig.10, curve 7), then the initial charge also reaches the maximum value. Under different initial conditions, the smaller charge is trapped first (intermediate curves between 7 and 8, Fig.10).

3.2. Compensation of charge losses with the use of a voltage source

The charge losses are compensated with the use of a voltage source by connecting the source for a short time to one capacitor only (see Fig. 1f). The charge losses on the second capacitor are compensated owing to the current flowing through the load resistance R in the process of generation with modulation of the capacitances. Breaux [37] considered another method: the charging of both capacitors. In this case, however, highly accurate synchronization of two switches is needed because even a small delay in commutation of switches leads to significant reduction of the generation efficiency.

The recharging voltage pulse should be applied at $V_1(t) < V_0$ and it should be finished at $C_1(t) = C_{max}$. An example of the optimum synchronization of the switch connecting the source V_0 in agreement with the capacitance modulation periods for the case of the lateral antiphase shift of the moving electrodes of the capacitors is shown in Fig. 15. Here the period of charging pulses T_{ch} was less than time constant of charge losses, no pronounced charge decay at $t < T_{ch}$ was observed, see Fig.15b.

When a series of recharging pulses is applied to compensate charge losses one can see the additional effect of charge growth by a factor of two compared to the case of ideal generator (Fig.15b) and corresponding growth of V_{min} value up to $V_{min} = V_0$ (Fig.15a).

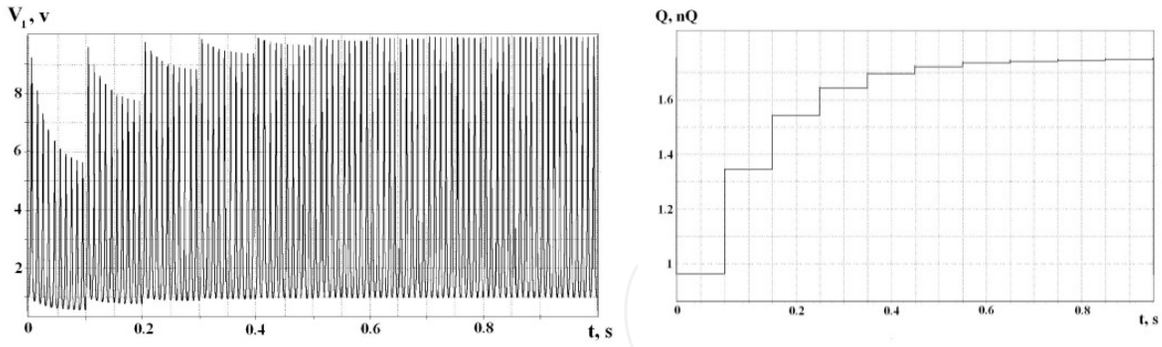

a. b.

Figure 15. Example of solving the problem of compensation of charge losses by recharging the capacitor from a voltage source. Mode of the lateral shift of the capacitor plates: (**a**) voltage on the first capacitor; (**b**) total charge. Recharging pulse duration 10 μs, amplitude 1 V, supply period 100 ms, number of cycles per the period $N = 10$, frequency 100 Hz, $C_{min} = 87.6$ pF, $\eta = 10$, $R = 2\ 10^8\ \Omega$, and $r = 10^{12}\ \Omega$.

Therefore, in this case the maximum energy transferred to the load resistance is greater than the energy of ideal generator by a factor of 4, and of single-capacitor generator (2) by a factor of 2; in the limit (at $\eta >> 1$) it tends to the value $C_{max}V_0^2\ \eta$ (see Fig. 10, curve *6*).

Thus, the use of a switch performing synchronous recharging of the capacitor C_1, in addition to compensation of charge losses, increases the charge to the limiting value $2C_{max}V_0$, which involves an increase in the generated energy up to values exceeding the energy generated by the ideal generator by a factor of 4. Note that similar features are also observed for the two-capacitor generator in vibration out-of-plane mode, leading to an even more dramatic increase in the generator power in this case (cf. curves 5 and 6 in Fig. 10).

4. Experimental studies of two-capacitor rotational generator

To prove the possibility of electric energy generation under the action of mechanical forces with highly efficient utilization of the charge injected into the generator, we performed experimental studies using a macroscopic model of two-capacitor generator consisting of two stator plates and rotor plate located exactly between them. Each plate was metalized and divided into 12 sectors in such a way as to provide the central plate with the two series of the connected capacitors modulated in antiphase when central plate is rotating. The area of the electrodes was 25 cm^2. The moving electrode was fixed on the shaft of a d. c. motor rotated with a frequency of the order of 1–50 Hz, therefore, the capacitor modulation frequency was 10–600 Hz. All plates were insulated from the body and shaft of the motor with the use of insulators having a high resistance (above 100 GΩ). The gap between the plates was 100–200 μm, the capacitance C_0 had the order of 250–350 pF, and the modulation factor was η = 1.8–3.5; these parameters were determined by independent measurements. The current through the load resistance $I(t)$ and the voltage on it $V(t)$ were measured by a digital oscilloscope using the matching circuit.

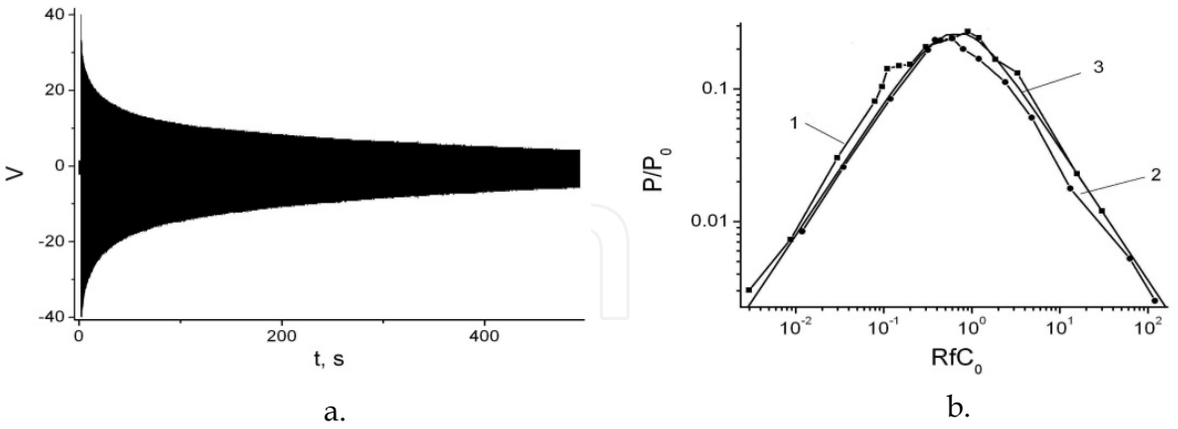

Figure 16. Experimental studies of two-capacitor generator: (**a**) - relaxation of voltage oscillations in the load resistance (C_0 = 300 pF, η = 1.8, R = 10 MΩ, and f = 400 Hz), (**b**) - characteristic loading curves of the ideal generator: f = 400 Hz (*1*), f = 100 Hz (C_0 = 300 pF and η = 1.8) (2), and calculation by the proposed model (*3*).

The oscillogram characterizing energy generation is shown in Fig. 16a. A charge of 2 10^{-8} C was initially injected at the time t = 0 into this structure by a short pulse of voltage equal to 80 V. After that, the flow of the current of up to 8 μA (acting value) through the load resistance R = 10 MΩ in the process of rotation of the moving electrode with the effective frequency of 400 Hz is determined by this charge. The initial time of voltage redistribution is of order $RC_0 = 3 \cdot 10^{-3}$ s, after that dynamically equilibrium mode of generation is established. Therefore, the measured initial amplitude of the voltage on the load resistance R (e.g., 40 V, based on the data in Fig. 16a) was used to calculate the power of the ideal generator in this mode on the basis of the proposed experimental model. Initial charging of the capacitors ensures energy generation for a long time (up to 1000 s). During this time, more than 4 10^5 cycles of energy conversion with the use of this charge take place, and the Joule energy released on the load resistance is much greater than the energy spent on initial charging of the generator capacitors. Based on the time constant of charge decay, we can easily estimate the leakage resistance; for the circuit considered, it is approximately 10^{12} Ω. The power developed by the generator with a 80-V starting voltage was 1 mW.

To confirm the main result of the developed generator model, i.e., the universal character of the dependences of the generated power on the load resistance R, we studied the specific features of energy generation at the initial stage of the process when the leakages could be neglected (in this period, the current amplitude is close to its value for the ideal generator). The loading curves plotted in the RfC_0–P/P_0 coordinates for different modulation frequencies of the generator capacitances were found to be almost coincident, i.e., to have a universal character and also to agree well with the model described above (Fig. 16b). Moderate disagreement is explained by a small difference in the modulation factors of two capacitors.

5. Peculiarities of microgenerators operation with vibrations of moving electrode in submicron gap above the surface of ferroelectric-metal structure

A technology of mutual shifting (vibration) of the surfaces of the microcircuit components in the submicron range was developed during the last 5–7 years in modern microelectronics, namely, in its most intensely developing direction: MEMS, e.g., gyroscopes, generators, frequency stabilizers, high-frequency filters. Recently we have demonstrated the possibility of use the nanogaps in electromechanical energy conversion for applications in micromotors and actuators [40-42], which is promising for use in inverse mechanic-to-electricity energy transformation also.

The characteristic feature of operation of electrostatic capacitance microgenerators, the capacitors of that having the structure consisting of substrate – metal - thin ferroelectric layer – moving electrode, is the possibility of creation of high electric field densities in the submicron gap between the surfaces of ferroelectric and moving electrode. Thus, high energy of electric field is stored, which is transformed then into the current. In this structure thin ferroelectric with high ε (more than 1000) plays a role of damping layer to supress a breakdown in the air gap, because the breakdown is controlled here by breakdown field strength of the ferroelectric (more than 10^7 V/m). Because the field strength distribution in the layers of the structure is inversly proportional to their ε ratio then the major portion of voltage is applied to the gap and the field in ferroelectric is much less than its breakdown value, even at high V. Therefore, the breakdown does not occure at high field strength in the gap reaching 10^{10} V/m at the gaps of order 10-100 nm and votages of 100 V, according to our experimental data.

The expressions for electric field strength in the gap E_1 and in the ferroelectric film E, and for the energy stored in the structure are the following:

$$E_1 = \frac{V}{d/\varepsilon + d_1}, \quad E = E_1/\varepsilon, \quad W = \frac{\varepsilon_0 V^2}{2(d/\varepsilon + d_1)} \ . \tag{45}$$

At $d_1 >> d/\varepsilon$, the following expressions are always true in the field of parameters listed above:

$$E_1 \approx \frac{V}{d_1}, \quad E \approx \frac{V}{\varepsilon d_1}, \quad W \approx \frac{\varepsilon_0 V^2}{2d_1} = \frac{\varepsilon_0 V}{2} E_1 = \frac{\varepsilon_0 d_1 E_1^2}{2}. \tag{46}$$

Thus the maximum energy generated per one sycle could reach 1-4 J/m^2 during the operation of microgenerators at submicron gaps. At low frequencies of order 10-100 Hz the output power could reach up to 10-40 mW/cm^2. This estimate is true for all types of capacitance generators discribed above, in spite of a number of differencies in various types of their implementation.

6. Discussion and conclusions

1. The analysis of general laws of operation of microgenerators based on the use of multi-layer structure consisting of electrode – thin dielectric - air gap – moving electrode has

been performed taking into account the oscillatory motions with modulation of both the electrodes overlap area (including a rotational motion) and interelectrode gap.

2. It was shown that the use of the submicron gaps in these microgenerators gives rise to considerable increase of output power. To achieve high energy output of these microgenerators it is necessary to have high values of maximal capacitance of generating element C_{max} and electric field strength in the interelectrode gap. These generators can develop a power of 40 mW/cm^2 and more for the range of low-frequency vibrations characteristic of the vibrations of environment without the use of voltage sources.

   The closest manufactured analogs of such generators are electret in-plane devices (with lateral shift of moving electrode). They have rather large sizes (about 20*20 mm^2) and small specific power (of order 100 μW/cm^2) despite the fact that the value of power was considerably increased by means of multiple overlapping of strips in interdigitated comb structure (see [5]) of the generator with high displacements (of about 1 mm) in resonance mode of operation [36]. It should be noted that these devices have large interelectrode gaps (more than 20 μm), which prevent the essential decrease of the sizes of generators to reach the values needed for the microelectronics. Therefore, we believe that the only alternative to solve the problem is the development of out-of-plane (vibration) constructions of generators.

3. The mathematical model of the generators was developed, and the numerical solutions describing the process of generation were derived. The universal type of these solutions was confirmed, and the analytical description of the output maximum power in dependence of capacitance modulation depth was carried out.

   The main parameters controlling the efficiency of electret generator operation were determined to be the ratio of charge built in dielectric layer to its geometric capacitance $V_p=Q_p/C_F$ and the value of mean capacitance of air gap C_1. It was shown that for two-capacitor capacitance generators these parameters are the values of maximum capacitance C_{max} and capacitance modulation depth η.

4. Unlike the one-capacitor prototype it was shown that for these generators it is not necessary to recuperate the charge in each cycle of power generation. For the electret generator there is no need at all to turn on the source to compensate charge losses. However, unlike the electret generator working in the current mode, to enlarge the output power it is necessary to use the switch synchronized with the certain phase of oscillations to short-circuit the plates of capacitor to eliminate the parasitic induced charge.

   There is no need to renew the charge at each cycle of power generation for two-capacitor generator in which the charge serves as "working medium" for production the electric power. It is necessary to compensate only small charge losses arising due to leakage currents in the capacitors.

It was determined that for the charge recuperation there is no need to connect the charge sources to each capacitor, it is enough to connect the source only to one of the capacitors. It

can be the current source (connected permanently) or the voltage source (connected for a short period of time in a certain phase of capacitance alteration and periodically after the high enough number of energy transformation cycles). In this case one can use the feedback circuit utilizing a small part of output energy for the recuperation of the initial charge.

Author details

Igor L. Baginsky and Edward G. Kostsov
Institute of Automation and Electrometry, Russian Academy of Sciences, Russia

7. References

[1] Roundy S, Wright P K, Rabaey J (2003) A study of low level vibrations as a power source for wireless sensor nodes. Computer Communs. 26: 1131-1144.
[2] Stephen N G (2006) On energy harvesting from ambient vibration. J. Sound Vib. 293: 409–425.
[3] Miyazaki M., Tanaka H, Ono G, Nagano T, Ohkubo N, Kawahara T (2004) Electric-energy generation using variable-capacitive resonator for power-free-LSI. IEICE Trans. Electron. E87: 549–555.
[4] Mitcheson P D, Miao P, Stark B H, Yeatman E M, Holmes A S, Green T C (2004) MEMS electrostatic micropower generator for low frequency operation. Sensors Actuators. A115:.523–529.
[5] Baginsky I L, Kostsov E G (2002) The possibility of creating a microelectronic electrostatic energy generator. Optoelectronics, Instrumentation and Data Processing. No.1: 89-102.
[6] El-Hami M, Glynne-Jones P, White N M, et al. (2001) Design and fabrication of a new vibration based electromechanical power generator. Sensors Actuators. A92: 335–342.
[7] Meninger S, Mur-Miranda J, Lang J, et al. (2001) Vibration to electric energy conversion. IEEE Trans. Very Large Scale Integration (VLSI) Syst.. 9: 64–76.
[8] Roundy S, Wright P K (2004) A piezoelectric vibration based generator for wireless electronics. Smart Mater. Struct.. 13: 1131–1142.
[9] Du Toit N E, Wardle B L, Kim S-G (2005) Design considerations for MEMS-scale piezoelectric mechanical vibration energy harvesters. Integrated Ferroelectrics. 71: 121–160.
[10] Chen C-T, Islam R A, Priya S (2006) Electric energy generator, ultrasonics, ferroelectrics and frequency control. IEEE Trans. Ultrasonics, Ferroelectrics Freq. Control, 53: 656–661.
[11] Dragunov V P, Kostsov E G (2009) Specific features of operation of electrostatic microgenerators of energy. Optoelectronics, Instrumentation and Data Processing. 45: 234–242.
[12] Beeby S P, Tudor M J, White N M (2006) Energy harvesting vibration sources for mycrosystems applications. Meas. Sci. Technol. 17: R175-R195.

[13] Lueke J, Moussa W A (2011) MEMS-based power generation techniques for implantable biosensing applications. Sensors. 11: 1433-1460.
[14] Mitcheson P D, Sterken T, He C, Kiziroglou M, Yeatman E M, Puers R. (2008) Electrostatic microgenerators. Meas. Cont. 41: 114-119.
[15] Moore A D, Ed. (1973) Electrostatics and its application. Wiley: N. Y. 481 p.
[16] Chang J, Kelly A J, Crowley J M, Ed. (1995) Handbook on electrostatic processes. Marcel Dekker Inc.: N.Y.
[17] Sessler G M, West J E (1987) Electrets, 2nd. ed. Topics in Applied Physics 33. Springer-Verlag.
[18] Chiu Y, Kuo C T, Chu Y S (2007) Design and fabrication of a micro electrostatic vibration-to-electricity energy conventer. Microsys. techn.-micro-nanosys.-inf. storage and processing systems. 13: 1663-1669.
[19] Basset P, Galayko D, Paracha A M, Marty F, Dudka A, and Bouroina T (2009) A bath fabricated and electret-free silicon electrostatic vibration energy harvester. J. Mictomech. Microeng. 19: 115025-115037.
[20] Hoffmann D, Folkmer B, Manoli Y (2009) Fabrication, characterization and modelling of electrostatic micro-generators. J. Micromech. Microeng. 19: 094001-094012.
[21] Kiziroglou M E, He C, Yeatman E M (2009) Rolling rod electrostatic microgenerator. IEEE Trans. Industrial Electron. 56: 1101-1108.
[22] Roundy S, Wright P K, Pister K S J (2002) Micro-electrostatic vibration-to-electricity converters. Proc. IMECE, November 17-22: New Orleans, Louisiana, 1-10.
[23] Baginsky I L, Kostsov E G, Sokolov A A (2010) Electrostatic microgenerators of energy with a high specific power. Optoelectronics, Instrumentation and Data Processing. 46: 580–592.
[24] Potter M D (2004) Electrostatic based power source and method thereof. US patent 6750590 B2.
[25] Naruse Y, Matsubara N, Mabuchi K, Izumi M, Suzuki S (2009) Electrostatic micro power generation from low-frequency vibration such as human motion. J. Micromech.Microeng. 19: 094002-094006.
[26] Grachevski S M, Funkenbush P D, Jia Z, Ross D S, Potter M D (2006) Design and modeling of a micro-energy harvester using embedded charge layer. J. Micromech. Microeng. 16: 235-241.
[27] Mizuno M, Chetwynd P G (2003) Investigation of resonance microgenerator. J.Micromech.Microeng. 13: 209-216.
[28] Okamoto H, Suzuki T, Mori K, Cao Z, Onuki T, Kuwano H (2009) The advantages and potential of electret-based vibration-driven micro energy harvesters. Int.J.Energy Res. 33: 1180-1190.
[29] Boland J, Chao Y H, Suzuki Y, Tai Y C (Jan. 19–23, 2003) Micro electret power generator. Proc. MEMS'03. Kyoto, Japan. 538–541.
[30] Masaki T, Sakurai K, Yokoyama T, Ikuta M, Sameshima H, Doi M, Seki T, Oba M. (2011) Power output enhancement of a vibration-driven electret generator for wireless sensor applications. J. Micromech. Microeng. 21: 104004- 104009.

[31] Ma W, Zhu R, Rufer L, Zohar Yi, Wong M (2007) An integrated floating-electrode electric microgenerator. J. Microelectromech. Sys. 16: 29-37.
[32] Mahmoud M A, El-Saadany E F, Mansour R R (Nov. 29 - Dec. 1, 2006) Planar electret based electrostatic micro-generator. The Sixth International Workshop on Micro and Nanotechnology for Power Generation and Energy Conversion Applications. Berkeley, U.S.A.: 223-226.
[33] Lo H, Tai Y-Ch (2008) Parylene-based electret power generators. J. Micromech. Microeng. 18 104006 – 104014.
[34] Suzuki Y (2011) Recent progress in MEMS electret generator for energy harvesting. IEEJ Trans. 6: 101–111.
[35] Lo H-W, Tai Y-Ch (2009) Electret power generator. US patent 0174281 A1.
[36] Sakane Y, Suzuki Y, Kasagi N (2008) The development of a high-performance perfluorinated polymer electret and its application to micro power generation. J. Micromech. Microeng. 18: 104011-104017.
[37] Breaux O P (1978) Electrostatic energy conversion system. US patent 4127804.
[38] Baginsky I L, Kamyshlov V F, Kostsov E G (2011) Specific features of operation of a two-capacitor electrostatic generator. Optoelectronics, Instrumentation and Data Processing. 47: 100 – 120.
[39] Lines M, Glass A (1977) Principles and Applications of Ferroelectrics and Related Materials. Oxford: Oxford University Press.
[40] Baginsky I L, Kostsov E G (2003) High-energy capacitive electrostatic micromotors. J. Micromech. Microeng. 13: 190–200.
[41] Baginsky I L, Kostsov E G (2004) Electrostatic micromotor based on ferroelectric ceramics. J. Micromech. Microeng. 14: 1569–1575.
[42] Baginsky I L, Kostsov E G (2007) High energy output MEMS based on thin layers of ferroelectric materials. Ferroelectrics. 351: 66–78.